

The mysterious long-range transport of giant mineral dust particles

Article

Published Version

Creative Commons: Attribution-Noncommercial 4.0

Open Access

van der Does, M., Knippertz, P., Zschenderlein, P., Harrison, G. and Stuut, J.-B. (2018) The mysterious long-range transport of giant mineral dust particles. *Science Advances*, 4 (12). eaau2768. ISSN 2375-2548 doi:
<https://doi.org/10.1126/sciadv.aau2768> Available at
<https://centaur.reading.ac.uk/80426/>

It is advisable to refer to the publisher's version if you intend to cite from the work. See [Guidance on citing](#).

To link to this article DOI: <http://dx.doi.org/10.1126/sciadv.aau2768>

Publisher: American Association for the Advancement of Science

All outputs in CentAUR are protected by Intellectual Property Rights law, including copyright law. Copyright and IPR is retained by the creators or other copyright holders. Terms and conditions for use of this material are defined in the [End User Agreement](#).

www.reading.ac.uk/centaur

CentAUR

Central Archive at the University of Reading

Reading's research outputs online

ATMOSPHERIC SCIENCE

The mysterious long-range transport of giant mineral dust particles

Michèle van der Does^{1*}, Peter Knippertz², Philipp Zschenderlein²,
R. Giles Harrison³, Jan-Berend W. Stuut^{1,4}

Giant mineral dust particles (>75 μm in diameter) found far from their source have long puzzled scientists. These wind-blown particles affect the atmosphere's radiation balance, clouds, and the ocean carbon cycle but are generally ignored in models. Here, we report new observations of individual giant Saharan dust particles of up to 450 μm in diameter sampled in air over the Atlantic Ocean at 2400 and 3500 km from the west African coast. Past research points to fast horizontal transport, turbulence, uplift in convective systems, and electrical levitation of particles as possible explanations for this fascinating phenomenon. We present a critical assessment of these mechanisms and propose several lines of research we deem promising to further advance our understanding and modeling.

INTRODUCTION

About 30 years ago, scientists first observed so-called giant (>75 μm in diameter) wind-blown mineral dust particles at large (>10,000 km) distances from their source (1). These sand-sized mineral aerosols or dust particles, the largest of which (>200 μm) were all individual quartz grains, were transported from Asia to the remote Pacific Ocean. In Europe, giant dust particles were found >4000 km from their Saharan source (2), and dust particles up to 300 μm in diameter were sampled during aircraft campaigns over northwestern Africa (3). In marine sediment traps, positioned underneath the main Saharan dust plume in the Atlantic Ocean, giant particles are dominated by large quartz particles >100 μm , found at distances up to 4400 km from the west African coast (4).

The Sahara is currently the largest single source of wind-blown sediments. Transport of Saharan dust across the Atlantic Ocean is subject to seasonal atmospheric changes in wind systems, blowing at different altitudes. In winter, low-level dust is carried toward the Atlantic with the northeasterly trade winds, or Harmattan, at altitudes between 0 and 3 km (5). In summer, the Saharan Air Layer (SAL) dominates dust transport. Upon reaching the west African coast, the SAL encounters a cool marine air mass that lifts the warm, dusty air to altitudes up to a maximum of 5 to 7 km (5–7). Wind velocities of up to 25 m s^{-1} associated with the Atlantic extension of the African easterly jet can lead to fast westward transport, particularly around 4 km (6, 8).

It is often assumed that the particle size of long-range transported mineral dust does not exceed 20 to 30 μm (9–12), and climate model simulations often limit particle diameters to only <10 μm (13). However, the incorporation of coarse particles is important as the radiative effect of dust is especially sensitive to the coarse dust mode. Coarse particles reduce the single-scattering albedo of shortwave radiation, increasing radiative absorption (3), and enhance the absorption of longwave radiation (14), possibly causing a net atmospheric warming as shown by Kok *et al.* (15). This latter study (15) also demonstrated a substantial effect on the atmospheric radiative balance when larger particles up to 20 μm are incorporated into climate models. If giant dust

particles (>75 μm) would be considered, then the effects on atmospheric radiation budgets could be tremendous. In addition, the underrepresentation (or nonrepresentation) of particles larger than 10 μm in climate models and the distance these particles can travel affect total deposition fluxes over land and ocean. Giant mineral dust particles also play a role in the ocean carbon cycle, as they have a large ballasting potential for marine organic aggregates, making these aggregates denser and therefore aiding the transport of organic matter to the deep ocean (16). In addition, they influence cloud microphysics by acting as giant cloud condensation nuclei, which can accelerate the hydrological cycle through increasing precipitation rates (17). This demonstrates why a mechanism explaining the long-range transport of giant dust particles is urgently needed.

RESULTS

New evidence for long-range transport of giant dust particles

Here, we present new data from the same trans-Atlantic transect as van der Does *et al.* (4), this time collected directly from the atmosphere by Modified Wilson and Cooke (MWAC) samplers (see Materials and Methods), mounted on moored dust-collecting surface buoys at two stations in the tropical North Atlantic Ocean. The passive air samplers collected one discrete sample during periods between 2013 and 2016, comprising 281 to 432 days (Table 1) at approximately 3 m above sea level. These samples show giant dust particles (>75 μm ; Fig. 1) that were collected at 2400 and 3500 km, respectively, from the west African coast at sampling stations M3 and M4 (Fig. 2). These are mostly well-rounded quartz particles up to 450 μm in diameter, with what appears to be high aspect ratios. As atmospheric samples, these sand-sized dust particles can only have been carried there by the wind. This observation adds further evidence to the ability of the atmosphere to transport giant particles over very long distances.

The main reason why climate models do not incorporate dust particles >10 μm , despite the growing evidence for their existence far away from sources suggesting substantial residence times in the atmosphere, is related to the physical laws on which the models are based. The settling speed of small particles in air is usually calculated using equations based on Stokes' law (10, 18). Settling velocities for particles >20 μm are overestimated by Stokes' law due to turbulence created by the falling of larger particles and are therefore determined empirically (10, 19).

¹NIOZ–Royal Netherlands Institute for Sea Research, Department of Ocean Systems, and Utrecht University, Texel, Netherlands. ²Institute of Meteorology and Climate Research, Karlsruhe Institute of Technology, Karlsruhe, Germany. ³Department of Meteorology, University of Reading, Reading, UK. ⁴Department of Earth Sciences, Faculty of Science, Vrije Universiteit Amsterdam, Netherlands.

*Corresponding author. Email: mdoes@nioz.nl

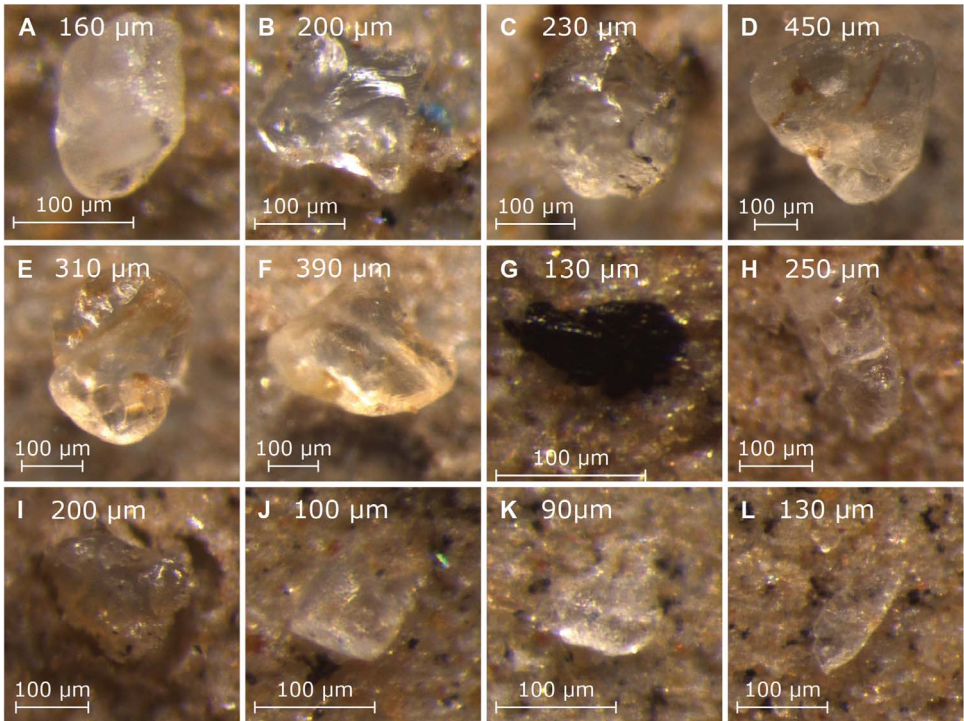


Fig. 1. Giant mineral dust particles sampled by the MWAC samplers at M3 (12°N, 38°W) and M4 (12°N, 49°W) in 2014 and 2015, with their approximate diameters. (A to C) 2014-M3; (D to F) 2014-M4; (G to I) 2015-M3; (J to L) 2015-M4.

Table 1. Sampling duration of MWAC samplers on the dust-collecting buoys at M3 and M4 (Fig. 2), together with statistics on the colocated wind measurements.						
	Sampling start	Sampling end	Days sampled	Minimum wind velocity (m s ⁻¹)	Maximum wind velocity (m s ⁻¹)	Average wind velocity (m s ⁻¹)
2014-M3	24 November 2013	01 September 2014	281	1.9	13.6	8.7 ± 2.0
2014-M4	28 November 2013	27 January 2015	425	4.5	14.2	9.1 ± 1.8
2015-M3	22 November 2015	29 March 2016	432	0.9	12.7	6.7 ± 1.7

Using the formula from Bagnold (19), we compare the settling velocities of giant mineral dust particles of 100, 200, and 300 μm (Table 2). These data show that, with such rapid settling velocities, it is not possible for giant particles to reach the sampling sites at 2400 and 3500 km from the west African coast (Fig. 2), even at high wind velocities of 25 m s⁻¹. Some additional mechanisms are needed to keep these dust particles aloft.

Potential mechanisms

Several studies suggest such mechanisms including atmospheric vertical mixing (18, 20, 21) or large dust storms and turbulence (1, 9, 11), but the capacity of these mechanisms for long-range transport of giant dust particles over the ocean has not been explored. In addition, the shape of the mineral dust particles can influence their deposition, with aspherical particles having lower settling velocities than more spherical particles (22, 23). However, this does not seem to have a large effect on the giant dust particles observed at our Atlantic sampling locations, as these are almost exclusively spherical quartz minerals (Fig. 1).

Here, we provide an integral discussion of the potential of four different mechanisms that can facilitate long-range transport of giant particles. First, strong winds causing fast horizontal transport greatly enhance the distance over which the dust travels. Second, transport of individual large dust particles is further aided by strong turbulence, keeping them in suspension for a longer time (24), although this could also have a negative effect on the dust particles, causing them to settle even quicker. Third, particle charge affects their dynamics and, for negatively charged particles, can offset a particle’s weight in a downward-directed electric field, so keeping it aloft for longer (25, 26). Last, thunderstorms or tropical cyclones can carry dust particles to great heights, strongly increasing their horizontal travel distance if the particles can leave the storm through the anvil or upper-level outflow region without being rained out. This mechanism will be particularly effective when multiple uplift cycles are encountered along active areas such as the intertropical convergence zone (ITCZ).

In the following, we provide a plausibility analysis of these four factors to test whether they can explain our new observations of

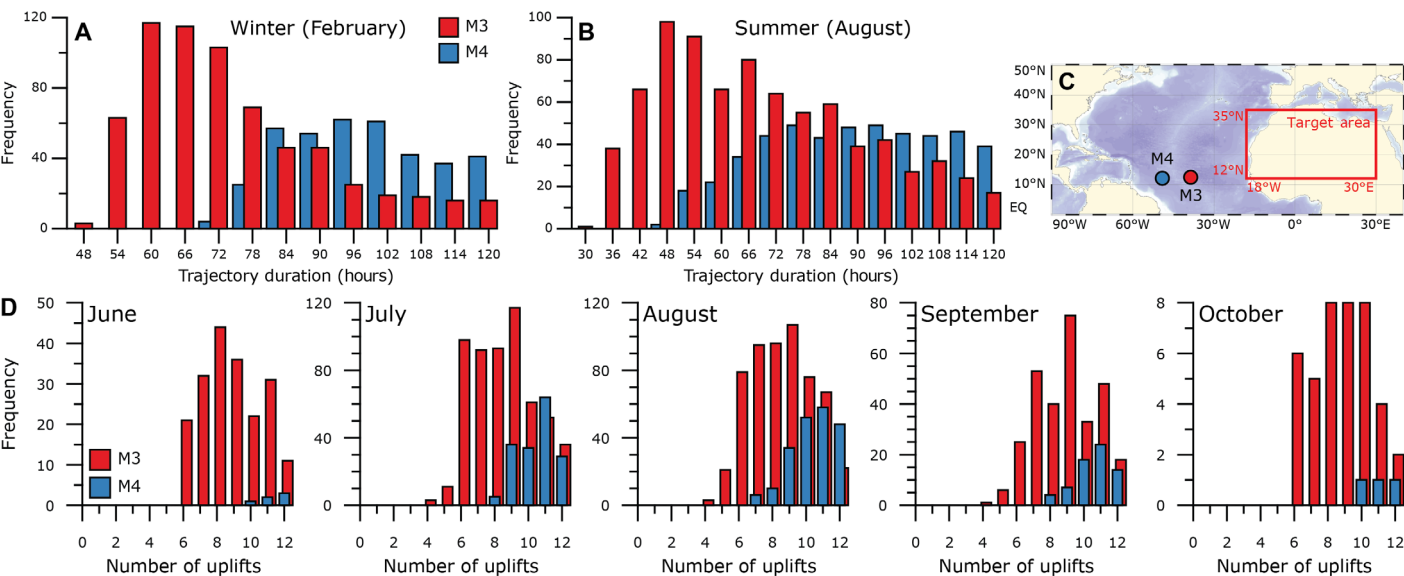


Fig. 2. Seasonality of atmospheric transport from Africa to the buoy sites. Distribution of travel times for backward trajectories from buoys M3 (red) and M4 (blue) to the target area (C), for February (A) and August (B). (D) Frequency of the minimum number of deep convective uplift cycles needed for a 100- μm particle to travel from the target area (C) to the sampling buoys M3 (red) and M4 (blue), assuming a constant sedimentation velocity of 400 mm s^{-1} (Table 2), for June to October. All computations are based on ERA-Interim data during the 10-year period 2006 to 2015.

Table 2. Settling velocities after Bagnold (19) and estimates of traveled distance based on favorable summer (strong winds and elevated dust) and winter (lower wind speeds and elevation) conditions.			
Particle size (μm)	Settling velocity (mm s^{-1})	Summer: Traveled distance at 25 m s^{-1} winds from 7-km altitude	Winter: Traveled distance at 10 m s^{-1} winds from 3-km altitude
100	400	438 km	75 km
200	1000	175 km	30 km
300	1500	117 km	20 km

giant dust particles. We will discuss winter and summer situations separately.

Winter scenario

In boreal winter, dust transport occurs at lower altitudes and at lower wind speeds (Table 2). There is insufficient convection over the sampling area to aid the long-range transport of dust particles, as the ITCZ is shifted southward (27). Backward trajectory calculations for February (see Materials and Methods) show that simple horizontal particle transport (no settling) within the boundary layer, where horizontal winds are fastest, would still take at least 48 hours to reach M3 and at least 72 hours to reach M4 (Fig. 2A). Transport at higher levels is unlikely, as winds become increasingly more westerly with height (28). Assuming the sedimentation velocities for particles of $100\text{ }\mu\text{m}$ given in Table 2, the shortest travel time to M3 and M4 would correspond to a total vertical sedimentation of ~ 70 and 100 km , respectively, strongly suggesting that other mechanisms must be involved. Fast horizontal transport events will be characterized by strong winds over the ocean but often also over land, as these tend to be associated with synoptic-scale subtropical highs (29), leading to large dust

emissions. Given that transport is usually restricted to the boundary layer, we can assume highly turbulent conditions, stirred mechanically by high wind shear, even in the absence of buoyancy generation over the ocean. However, it is difficult to quantify the effect of turbulence on the likelihood of individual giant dust particles to stay suspended without any direct observations of this process. The third mechanism that may contribute to keeping giant particles aloft is via electrical forces. Many studies have found that atmospheric charging affects particle dynamics, with a vertical electrical force being able to potentially compensate a particle’s weight (25, 26). Renard *et al.* (26) found large particles ($>40\text{ }\mu\text{m}$) persisting over long distances over the Mediterranean region, without significant downwind trends in size. They speculated that this was due to particle charge, counteracting gravitational settling. Electric charge has also been shown to increase dust emission from source areas up to 10-fold (30, 31). Whether or not the electric field hinders or assists a particle in staying aloft depends on the relative polarity of the particle and the atmospheric electric field encountered. The downward-directed electric field always present in fair weather will drive positively charged particles downward, but the field direction can reverse in disturbed weather or during saltation

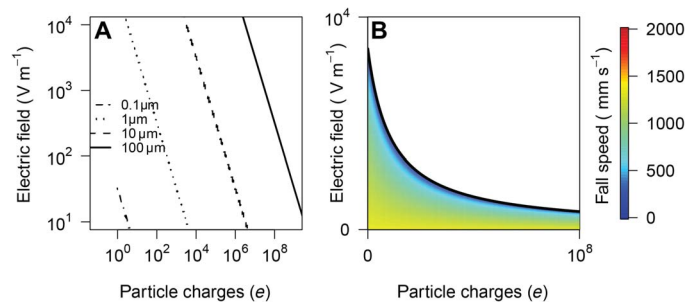


Fig. 3. Influence of charge and electric field on the net force on a particle. (A) Combination of particle charge and local electric field required for the magnitude of the electric force experienced by a particle to equal the particle's weight, for particles having diameters of 0.1, 1, 10, and 100 μm. (B) Fall speed for a 100-μm quartz particle for increasing electric field and particle charge (density of quartz = 2648 kg m⁻³, drag coefficient $C_D = 1.5$).

events (32) and particles can readily carry both polarities of charge, so an upward electrical force is possible. The initial charge generated at dust emission is lost within hours (25), but charged particles have still been detected far away from sources. For instance, during Hurricane Ophelia of October 2017, which brought large amounts of dust and smoke particles to the southern United Kingdom, appreciable negative charge was detected in the dust plume after a transport time of tens of hours (33), showing that charge is also generated during transport. The most likely reason is that particles are more or less continuously charging through collisions, a process called triboelectrification (32, 34). This effect is facilitated in an atmospheric layer that is characterized both by a high dust concentration and strong turbulence, exactly the kind of strong-wind situation described above, which would sustain electric fields sufficiently to reduce the fall speeds of highly charged particles. A further consequence of a system of particles is to reduce the air's electrical conductivity through removal of cluster ions, allowing the charge on the particle assembly to be sustained for longer than for an isolated charged particle.

Two factors together determine the electrical effect on a particle of a given size: the local atmospheric electric field and the particle charge. The atmospheric electric field varies appreciably between fair weather conditions ($E = -10^2$ V m⁻¹) and disturbed weather conditions such as convective clouds and thunderstorms in which substantial charge separation occurs meteorologically to generate strong electric fields of different polarities ($E = \pm \sim 10^4$ V m⁻¹). An individual particle's charge aloft can also cover a wide range, resulting from its interactions with other particles and cosmic ray-generated ions or, exceptionally, its internal radioactivity. Figure 3A shows the number of particle charges necessary for the electric force on the particle to have the same magnitude as a particle's weight in a range of typical atmospheric electric fields, that is, under which conditions it could become levitated. In the weak fair weather field (10^2 V m⁻¹), only the smallest particles are affected, with ~ 2 elementary charges (e) required. For larger particles, the number of charges and field required increases. In electric fields characteristic of disturbed weather ($\sim 10^4$ V m⁻¹), particles of 100 μm typically require 10^7 or 10^8 e to offset their weight and reduce the particle's fall speed (Fig. 3B). In situ measurements of individual particle charge aloft are not available for comparison, and related quantities near the surface are only poorly known, but charges found in dust devils are of $\sim 10^6$ e cm⁻³ (34) and resuspended dust on the order of 10^3 to 10^4 e per particle (or 10^{12} e cm⁻³) (32). Larger charges are likely for giant particles, scaling with particle area, but at very large charges and fields,

charge emission would prevent further electrification (35). One highly relevant factor is particle composition (30, 32), as it is known that mineralogy affects the charging of particles. The giant dust particles found at the buoys are mostly quartz (Fig. 1), and it is found experimentally that quartz particles may charge more easily than clay minerals [(32) and references therein]. Any electrically assisted transport would require the sustained or fortuitous presence of strongly electrified clouds and particle charges of the appropriate relative polarities. More laboratory, field, and numerical studies are needed to quantify this effect in a fully turbulent dust layer with interacting particles of different sizes.

Summer scenario

A fourth potential mechanism occurs during summer in the presence of ITCZ convection. Fastest horizontal transport [based on 6-hourly ERA-Interim three-dimensional wind fields (36); see Materials and Methods] at the latitude of the buoys (i.e., $\sim 12^\circ$ N) occurs within the African easterly jet (37), reducing the minimum transport time in August to M3 at 600 hPa to 30 hours and to M4 to 48 hours (Fig. 2B). This is substantially less than in winter, generally increasing the probability of giant dust particles reaching the sampling sites, consistent with the higher number of larger dust particles found in submarine sediment traps at our sampling sites in summer (4). As in winter, we would generally assume giant particles to only reach the buoys during the strongest wind situations as reflected in our trajectory computations. Because of the SAL being elevated, surface friction cannot help create turbulence as in winter. Therefore, the question arises whether the shear above or below the wind maximum is strong enough to mechanically stir the atmosphere. Dust radiative heating in the layer could potentially modify vertical stability to sustain turbulence and thus vertical motion. Given the high dust loadings typical for summer and assuming some level of turbulence, triboelectrification may also play a role, as indicated by balloon measurements from Cape Verde (25). In contrast to winter, however, the decoupling from the surface suggests overall lower levels of turbulence. Therefore, it is conceivable that vertical transport in convective systems is needed in addition to support long-range transport.

In summer, the buoys are close to the Atlantic ITCZ (27), where convection is frequent. In August, the tropical cyclone season also intensifies [e.g., (38)]. Convective cells can uplift individual particles to the high tropical tropopause at altitudes of about 15 km (37, 39, 40). Satellite observations have shown that dust particles can escape areas of deep convection and exit the systems from upper layers, although significant amounts are washed or rained out (41). Such transports have the disadvantage of lifting particles out of the strongest horizontal winds at mid-levels, which would increase the overall travel time. However, a little closer to the equator, a second wind maximum, the so-called tropical easterly jet, exists near the tropopause (37).

To test this effect, a simple experiment was conducted. Five-day backward trajectories were calculated (see Materials and Methods) that incorporate a forced, immediate uplift to the upper troposphere (at 150 hPa) simulating deep convection. Using a settling velocity of 400 mm s⁻¹ for a 100-μm dust particle (Table 2) (19), we calculated the number of times such a dust particle would have to be lifted to the tropopause and subsequently settle back to sea level to arrive at the mid-ocean sampling sites. The results reveal that summer conditions require the fewest uplift cycles to cover the source-to-sink distance: In July and August, a dust particle of 100 μm has a 1 in 400 chance of reaching sampling site M3 with only four repeated uplifts (Fig. 2D). Chances increase greatly with increasing amount of uplift cycles along the

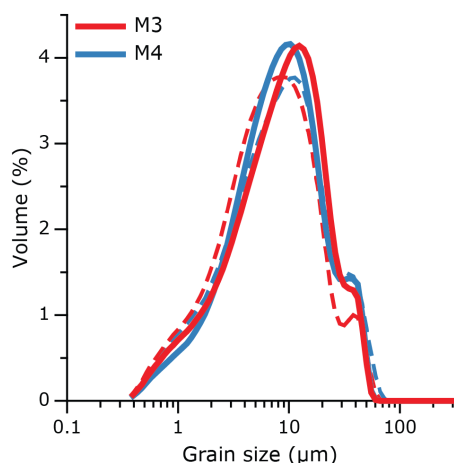


Fig. 4. Grain-size distributions of MWAC samples collected in 2014 (solid lines) and 2015 (dashed lines).

trajectory. For the same particle to reach M4, a minimum of seven uplift cycles would be required, which is reached in August on only a few occasions (Fig. 2D).

According to satellite estimates, every uplift cycle reduces the mass of dust by about a factor of 60, as 1.6% ($\pm 0.7\%$) of the Saharan dust layer mass can escape the deep convective cloud between 8 and 12 km (41). This would result in a minimum dilution of dust particles of nearly 1.3×10^7 to station M3 and 2.8×10^{12} to M4, as most of the dust uplifted by convection is removed by wet deposition (10, 41). Initial giant (37.5 to 300 μm) dust particle concentrations estimated by Ryder *et al.* (11) are up to 12,000 particles m^{-3} within 12 hours of uplift. These estimates suggest that this mechanism alone seems unlikely to explain the observed long-range transport, as the minimum number of uplift cycles would result in negligible concentrations of 7.9×10^{-4} and 3.2×10^{-9} dust particles per cubic meter of air at M3 and M4, respectively. Therefore, either the convection would need to be combined with effects of turbulence and charge or several convective uplifts would need to occur within the same long-lived convective system.

Possible scenarios for this re-entrainment in a convective cell are long-lived squall lines from West Africa that transport particles out through the stratiform region to the east and re-enter through the rear inflow jet (42). Such a scenario would also benefit from a strong African easterly jet and associated shear. An alternative mechanism is lifting in tropical cyclones, for example, up in the eyewall, out to the west of the system near the tropopause and re-integration after sedimentation to lower levels. This scenario would be more likely in areas of less shear, as shear tends to be detrimental to tropical cyclone development, but would benefit from the very long lifetime of tropical cyclones. However, both the convective uplift and the electric charge are affected by precipitation processes, as charge promotes the removal of dust by cloud droplets (25), and most dust uplifted by convection is deposited by wet deposition (10, 41). Therefore, convection and charging could also potentially work against each other.

DISCUSSION

We have presented evidence that giant mineral dust particles are transported through the atmosphere across the Atlantic Ocean, thousands of kilometers from their north African sources. We have evaluated four possible mechanisms that could aid this long-range transport.

The best option for dust particles to be transported over great distances is within the turbulent SAL in summer, as this elevated atmospheric layer facilitates conditions optimal for the proposed mechanisms. First, this air layer is characterized by strong winds (5–7), and turbulence created in this layer in combination with high particle concentrations allows for triboelectrification of dust particles, compensating the particles' weight. In summer, long-range transport can be further facilitated by deep convective clouds, lifting dust particles to the upper troposphere, also due to the more northern position of the ITCZ. Long-range transport of giant mineral dust particles in winter seems less likely, although data suggest that it does occur, albeit in a lower amount.

Our analysis has shown that highly optimal conditions need to be met to make the transport we observe possible, and many details about the mechanisms we investigated are still unquantified. More theoretical, laboratory, field, and modeling work is required to substantiate our estimates, and a more detailed study of dust collected at long distances from the source should give more information on the seasonality of giant particle transport and particle concentrations. We would like to propose several future research directions to further investigate the possibilities and constraints of the discussed mechanisms.

- 1) The dust-collecting buoys, which actively sample dusty air through a carousel of filters, will produce a time series of dust concentrations and giant particle counts, parallel to meteorological observations such as wind speed and wind direction, which will be crucial for the understanding of the magnitude of occurrence of long-range transport of giant particles.

- 2) In situ measurements of particle charge and electric fields in combination with dust particle size and concentrations would help the quantification of the effect that charge has on the horizontal transport distance of giant dust particles.

- 3) A more detailed meteorological analysis of, for example, the occurrence of large convective cells along the Saharan dust plume trajectory could quantify the possibility of the giant dust particles being transported by convective cells and whether some kind of re-entrainment into moving convective systems takes place that could enable particles to be uplifted several times in the same long-lived system.

- 4) More theoretical, field, laboratory, and modeling work on quantifying the effect of turbulence on the survival of giant particles could help to understand this process and the effect on the number of particles being transported over long distances.

- 5) Once there is a better understanding of the occurrence and effect of these mechanisms, then these should be incorporated into climate models and allow the long-range transport of giant mineral dust particles, rather than a priori restriction to the transport of particles $< 10 \mu\text{m}$. As a result of incorporating giant particles into Earth system models, many processes will be improved, in particular, estimations of the atmospheric radiative balance and, in turn, the atmosphere's global energy budget, which are highly affected by the coarse dust fraction.

MATERIALS AND METHODS

MWAC samplers

In conjunction with the sediment traps described in van der Does *et al.* (4), two moored dust-collecting surface buoys were deployed at two of the sampling stations, M3 (12.39°N, 38.63°W) and M4 (12.06°N, 49.19°W) (Fig. 2), for two consecutive years (Table 1). These buoys were equipped

with one MWAC (43) sampler each, a passive air sampler that sampled continuously over the time the buoys were deployed. Our MWAC samplers consisted of a plastic bottle with an inlet and outlet tube of 7.5 mm in diameter. They were installed vertically about 3 m above sea level, while a wind vane ensured windward orientation. The MWAC samplers have sampling efficiencies between 75 and 105% for dust with a median particle size of 30 μm , which means that, in some occasions, an oversampling would occur. However, Goossens and Offer (43) conclude that the MWACs are the least inefficient samplers. Sampling efficiency varies slightly with different wind speeds but without apparent trends (43). For sand-sized particles with median grain sizes between 132 and 287 μm , the samplers have slightly higher efficiencies of 90 to 120%, which are constant and independent of wind speed for velocities between 6.6 and 14.4 m s^{-1} (44). Maximum wind velocities at the sampling stations approximated 14 m s^{-1} (Table 1). We found these samplers to be best suited for our sampling purposes, as their sampling efficiencies are good, the mechanism is extremely simple, and the samplers are very inexpensive.

The MWAC samplers collected a discrete Saharan dust sample over the entire sampling period. Besides mineral dust, the samples inevitably also contained sea salts. These were removed by rinsing the sample bottle with Milli-Q water and subsequently filtering over a 25-mm polycarbonate filter with a pore size of 0.4 μm (2014 samples) and 47-mm polycarbonate filters with a pore size of 0.2 μm (2015 samples). These filters were then qualitatively analyzed with a light microscope for the presence of giant mineral dust particles and photographed. Grain-size distributions of the complete MWAC samples were obtained using a laser particle size analyzer Coulter LS13 320, using the method described by van der Does *et al.* (4) (Fig. 4). Figure 4 shows the limitations of this method of obtaining information on giant particles, which are present in numbers that are below the detection limit of the laser particle sizer, and thus not registered in the grain-size distributions, which show particles up to only 80 μm .

We have tried to eliminate any possible contamination of giant particles to our dust samples. Light-microscope analysis (Fig. 1) confirms the giant particles to be mineral dust and not, for example, plastic fragments from the sampling bottle, not salt crystals (which have a very typical cubic mineral shape), nor glass shards from glass beakers and petridishes (which would have very angular shape, with typical glass fracture features). In addition, we can see that some of these particles have some sort of iron coatings, typical for Saharan dust particles. Other sources of sediment can be excluded since these samples were collected in the middle of the Atlantic Ocean, directly from the air. Therefore, the possibility of contributions from the ocean or riverine input can be excluded.

The moored dust-collecting surface buoys are also equipped with a carousel of 24 filters through which a pump actively samples air, and as a result, the dust can be collected on these filters on a much higher resolution (45). Unfortunately, this active sampling proved to be unsuccessful as all the filters were retrieved ruptured, and future sampling campaigns will allow for a much more detailed study of the occurrence of giant mineral dust particles (seasonality, giant particle concentration in air, etc.). The sampling is done in parallel with meteorological observations such as wind speed and wind direction. In addition, future upgrades of the buoys will include wet deposition samplers.

Estimation of travel paths based on Stokes' law

Typically, dust is lifted to a maximum altitude of about 7 km within the SAL (5). If an individual 100- μm dust particle was uplifted to 6.5 km at

wind speeds of 25 m s^{-1} , and subject to a settling velocity of 0.4 m s^{-1} based on Stokes' Law (19), then it would be transported ~400 km horizontally before reaching sea level. This is only about halfway to the most eastern sampling station M1 (12°N, 23°W) (4), 700 km from the west African coast, demonstrating that horizontal transport alone is insufficient, by far, for the long-range transport of even larger dust particles, such that some additional mechanisms are needed to keep these dust particles aloft.

Trajectory calculation for giant mineral dust particles

Five-day backward trajectories were calculated using LAGRANTO (46, 47) for the 10-year period between 2006 and 2015 to obtain a robust climatological estimate. LAGRANTO is a Lagrangian trajectory analysis tool, which solves the following trajectory equation

$$\frac{d\vec{x}}{dt} = \vec{u}(\vec{x}) \quad (1)$$

With $\vec{x} = (\lambda, \phi, p)$ being the position vector in geographical coordinates (longitude, latitude, height in pressure coordinates) and $\vec{u} = (u, v, w)$ being the three-dimensional wind vector (zonal, meridional, and vertical). LAGRANTO is driven by 6-hourly ERA-Interim (36) three-dimensional wind fields. The trajectories were started every 6 hours at the locations of buoys M3 and M4 (see Fig. 2), resulting in a total of about 1200 trajectories per month. Trajectories that potentially carry dust are determined on the basis of their passage through a target region defined here as the area between 12°N and 35°N and between 18°W and 30°E (Fig. 2B).

Three types of experiments were conducted:

1) Transport within the boundary layer: In winter time, dust usually remains in the lowest 1.5 km (5, 23, 48). In this layer, the atmosphere is characterized by the near-surface northeasterly trade winds over the ocean. Fastest transport from Africa to M3 and M4 can be expected in this layer, as winds become increasingly westerly with height in winter (28). Therefore, to estimate the shortest possible traveling time (assuming no sedimentation), trajectories were started at 50 hPa above M3 and M4 and computed with the ERA-Interim three-dimensional wind fields. This was only done for February when wintertime dust reaches its westernmost extension over the ocean (49).

2) Transport within the SAL: In summer, fastest transport occurs within the SAL associated with the western extension of the African easterly jet with its core around 600 hPa. To test shortest possible travel times, we therefore computed trajectories starting from this level over M3 and M4 during August, when the jet reaches its northernmost position and is fully developed (50).

3) Transport affected by convective lifting: In summer, dust travels in the vicinity of the ITCZ and could therefore be lifted within convective updrafts. To estimate the effect of this on travel time, also taking into account sedimentation, a simple thought experiment was conducted. The vertical velocity (ω) field in ERA-Interim was modified to reflect the settling velocities of dust particles. A constant value of 400 mm s^{-1} (1.44 km hour^{-1}), typical for particles of 100 μm in diameter (19), was added globally. This settling velocity was converted into pressure coordinates, as ERA-Interim defines vertical velocities in Pascal per second using Eq. 2

$$\omega = -\rho g w \quad (2)$$

where ω is the vertical velocity in pressure coordinates, ρ is the density, g is the gravitational constant, and w is the vertical velocity in height coordinates. The density ρ was calculated using Eq. 3

$$\rho = \frac{p}{RT} \quad (3)$$

where p is pressure, R the ideal gas constant for dry air ($R_d = 287 \text{ J kg}^{-1} \text{ K}^{-1}$), and T is the temperature from the U.S. Standard Atmosphere (51).

When calculating backward trajectories, air parcels ascended rapidly due to the effect of sedimentation. Upon crossing the tropopause (defined here as 150 hPa), parcels were immediately set down to 950 hPa, mimicking the (backward) effect of a convective updraft. The number of convective updrafts needed for the parcel to reach the target region was counted. The winter months did not yield any notable results due to the predominance of westerlies at upper levels.

Charge effects

The effect of an electric force on the fall speed of a particle has been considered using a simple model of a spherical particle of radius r in a vertical electric field E , with weight W , an Archimedean upthrust U , an electric force F_E , and a drag force F_D . If the particle is moving downward but experiencing an upward electric force (due to carrying a negative charge in a downward-directed field, such as that in fair weather), then the balance of forces in equilibrium can be represented as

$$U + F_E + F_D = W \quad (4)$$

The ratio of U to W is given by the ratio of the densities of air ρ_a and the particle ρ_p , which is $\sim 1:1000$; hence, $U \ll W$ and U can be neglected. The drag force depends on the particle's projected area A ($= \pi r^2$), its fluid-relative speed v , and the drag coefficient C_D . Assuming a spherical particle carrying a charge q , the electric force can be written as qE , the drag force parameterized as $C_D \frac{1}{2} \rho_a v^2$; hence, the equilibrium description of Eq. 4 becomes

$$qE + C_D \frac{1}{2} \rho_a v^2 = \frac{4}{3} \pi r^3 \rho_p g \quad (5)$$

For calculation of v , C_D depends on the flow and the associated Reynolds number and typically varies from 0.5 to 1.5 for a smooth sphere.

SUPPLEMENTARY MATERIALS

Supplementary material for this article is available at <http://advances.sciencemag.org/cgi/content/full/4/12/eaau2768/DC1>

Data file S1. Data on backward trajectories and grain-size distributions.

REFERENCES AND NOTES

- P. R. Betzer, K. L. Carder, R. A. Duce, J. T. Merrill, N. W. Tindale, M. Uematsu, D. K. Costello, R. W. Young, R. A. Feely, J. A. Breland, R. E. Bernstein, A. M. Greco, Long-range transport of giant mineral aerosol particles. *Nature* **336**, 568–571 (1988).
- N. J. Middleton, P. R. Betzer, P. A. Bull, Long-range transport of 'giant' aeolian quartz grains: Linkage with discrete sedimentary sources and implications for protective particle transfer. *Mar. Geol.* **177**, 411–417 (2001).
- C. L. Ryder, E. J. Highwood, P. D. Rosenberg, J. Trembath, J. K. Brooke, M. Bart, A. Dean, J. Crosier, J. Dorsey, H. Brindley, J. Banks, J. H. Marsham, J. B. McQuaid, H. Sodemann, R. Washington, Optical properties of Saharan dust aerosol and contribution from the coarse mode as measured during the Fennec 2011 aircraft campaign. *Atmos. Chem. Phys.* **13**, 303–325 (2013).
- M. van der Does, L. F. Korte, C. I. Munday, G.-J. A. Brummer, J.-B. W. Stuut, Particle size traces modern Saharan dust transport and deposition across the equatorial North Atlantic. *Atmos. Chem. Phys.* **16**, 13697–13710 (2016).
- C. Tsamalis, A. Chédin, J. Pelon, V. Capelle, The seasonal vertical distribution of the Saharan Air Layer and its modulation by the wind. *Atmos. Chem. Phys.* **13**, 11235–11257 (2013).
- F. Chouza, O. Reitebuch, A. Benedetti, B. Weinzierl, Saharan dust long-range transport across the Atlantic studied by an airborne Doppler wind lidar and the MACC model. *Atmos. Chem. Phys.* **16**, 11581–11600 (2016).
- A. M. Adams, J. M. Prospero, C. Zhang, CALIPSO-derived three-dimensional structure of aerosol over the Atlantic basin and adjacent continents. *J. Climate* **25**, 6862–6879 (2012).
- M. Sarnthein, G. Tetzlaff, B. Koopmann, K. Wolter, U. Pflaumann, Glacial and interglacial wind regimes over the eastern subtropical Atlantic and North-West Africa. *Nature* **293**, 193–196 (1981).
- H. Tsoar, K. Pye, Dust transport and the question of desert loess formation. *Sedimentology* **34**, 139–153 (1987).
- C. S. Zender, H. Bian, D. Newman, Mineral dust entrainment and deposition (DEAD) model: Description and 1990s dust climatology. *J. Geophys. Res. Atmos.* **108**, (2003).
- C. L. Ryder, E. J. Highwood, T. M. Lai, H. Sodemann, J. H. Marsham, Impact of atmospheric transport on the evolution of microphysical and optical properties of Saharan dust. *Geophys. Res. Lett.* **40**, 2433–2438 (2013).
- J. F. Kok, E. J. R. Parteli, T. I. Michaels, D. Bou Karam, The physics of wind-blown sand and dust. *Rep. Prog. Phys.* **75**, 106901 (2012).
- N. Huneus, M. Schulz, Y. Balkanski, M. C. Krol, T. Takemura, C. S. Zender, Global dust model intercomparison in AeroCom phase I. *Atmos. Chem. Phys.* **11**, 7781–7816 (2011).
- S. Otto, M. De Reus, T. Trautmann, A. Thomas, M. Wendisch, S. Borrmann, Atmospheric radiative effects of an in situ measured Saharan dust plume and the role of large particles. *Atmos. Chem. Phys.* **7**, 4887–4903 (2007).
- J. F. Kok, D. A. Ridley, Q. Zhou, R. L. Miller, C. Zhao, C. L. Heald, D. S. Ward, S. Albani, K. Haustein, Smaller desert dust cooling effect estimated from analysis of dust size and abundance. *Nat. Geosci.* **10**, 274–278 (2017).
- H. Van der Jagt, C. Friese, J.-B. W. Stuut, G. Fischer, M. H. Iversen, The ballasting effect of Saharan dust deposition on aggregate dynamics and carbon export: Aggregation, settling and scavenging of marine snow. *Limnol. Oceanogr.* **63**, 1386–1394 (2018).
- R. Posselt, U. Lohmann, Influence of giant CCN on warm rain processes in the ECHAM5 GCM. *Atmos. Chem. Phys.* **8**, 3769–3788 (2008).
- H. Maring, D. L. Savoie, M. A. Izaguirre, L. Custals, J. S. Reid, Mineral dust aerosol size distribution change during atmospheric transport. *J. Geophys. Res. Atmos.* **108**, 8592 (2003).
- R. A. Bagnold, *The Physics of Blown Sand and Desert Dunes* (Methuen, 1941).
- J. Gasteiger, S. Groß, D. Sauer, M. Haarig, A. Ansmann, B. Weinzierl, Particle settling and vertical mixing in the Saharan Air Layer as seen from an integrated model, lidar, and in situ perspective. *Atmos. Chem. Phys.* **17**, 297–311 (2017).
- C. Denjean, F. Cassola, A. Mazzino, S. Triquet, S. Chevaillier, N. Grand, T. Bourrianne, G. Mombouisse, K. Sellegri, A. Schwarzenbock, E. Freney, M. Mallet, P. Formenti, Size distribution and optical properties of mineral dust aerosols transported in the western Mediterranean. *Atmos. Chem. Phys.* **16**, 1081–1104 (2016).
- W. Yang, A. Marshak, A. B. Kostinski, T. Várnai, Shape-induced gravitational sorting of Saharan dust during transatlantic voyage: Evidence from CALIOP lidar depolarization measurements. *Geophys. Res. Lett.* **40**, 3281–3286 (2013).
- J.-B. Stuut, M. Zabel, V. Ratmeyer, P. Helmke, E. Scheffé, Provenance of present-day eolian dust collected off NW Africa. *J. Geophys. Res.-Atmos.* **110**, D04202 (2005).
- L. Garcia-Carreras, D. J. Parker, J. H. Marsham, P. D. Rosenberg, I. M. Brooks, A. P. Lock, F. Marengo, J. B. McQuaid, M. Hobby, The turbulent structure and diurnal growth of the Saharan atmospheric boundary layer. *J. Atmos. Sci.* **72**, 693–713 (2015).
- K. A. Nicoll, R. G. Harrison, Z. Ulanowski, Observations of Saharan dust layer electrification. *Environ. Res. Lett.* **6**, 014001 (2011).
- J.-B. Renard, F. Dulac, P. Durand, Q. Bourgeois, D. Quentin, C. Denjean, D. Vignelles, B. Couté, M. Jeannot, N. Verdier, M. Mallet, In situ measurements of desert dust particles above the western Mediterranean Sea with the balloon-borne Light Optical Aerosol Counter/sizer (LOAC) during the ChArME campaign of summer 2013. *Atmos. Chem. Phys.* **18**, 3677–3699 (2018).
- N. Žagar, G. Skok, J. Triebbia, Climatology of the ITCZ derived from ERA Interim reanalyses. *J. Geophys. Res. Atmos.* **116**, 10.1029/2011JD015695 (2011).
- R. A. Tomas, P. J. Webster, Horizontal and vertical structure of cross-equatorial wave propagation. *J. Atmos. Sci.* **51**, 1417–1430 (1994).
- P. Knippertz, M. Tesche, B. Heinold, K. Kandler, C. Toledano, M. Esselborn, Dust mobilization and aerosol transport from West Africa to Cape Verde—A meteorological overview of SAMUM-2. *Tellus B* **63**, 430–447 (2011).
- F. Esposito, R. Molinaro, C. I. Popa, C. Molfese, F. Cozzolino, L. Marty, K. Taj-Eddine, G. D. Achille, G. Franzese, S. Silvestro, G. G. Ori, The role of the atmospheric electric field in the dust-lifting process. *Geophys. Res. Lett.* **43**, 5501–5508 (2016).

31. J. F. Kok, N. O. Renno, Enhancement of the emission of mineral dust aerosols by electric forces. *Geophys. Res. Lett.* **33**, 10.1029/2006GL026284 (2006).
32. R. G. Harrison, E. Barth, F. Esposito, J. Merrison, F. Montmessin, K. L. Aplin, C. Borlina, J. J. Berthelier, G. Déprez, W. M. Farrell, I. M. P. Houghton, N. O. Renno, K. A. Nicoll, S. N. Tripathi, M. Zimmerman, Applications of electrified dust and dust devil electrodynamics to martian atmospheric electricity. *Space Sci. Rev.* **203**, 299–345 (2016).
33. R. G. Harrison, K. A. Nicoll, G. J. Marlon, C. L. Ryder, A. J. Bennett, Saharan dust plume charging observed over the UK. *Environ. Res. Lett.* **13**, 054018 (2018).
34. W. M. Farrell, P. H. Smith, G. T. Delory, G. B. Hillard, J. R. Marshall, D. Catling, M. Hecht, D. M. Tratt, N. Renno, M. D. Desch, S. A. Cummer, J. G. Houser, B. Johnson, Electric and magnetic signatures of dust devils from the 2000–2001 MATADOR desert tests. *J. Geophys. Res. Planets* **109**, 10.1029/2003JE002088 (2004).
35. K. T. Whitby, B. Y. H. Liu, The electrical behaviour of aerosols, in *Aerosol Science*, C. N. Davies, Ed. (Academic Press, 1966).
36. D. P. Dee, S. M. Uppala, A. J. Simmons, P. Berrisford, P. Poli, S. Kobayashi, U. Andrae, M. A. Balmaseda, G. Balsamo, P. Bauer, P. Bechtold, A. C. M. Beljaars, L. van de Berg, J. Bidlot, N. Bormann, C. Delsol, R. Dragani, M. Fuentes, A. J. Geer, L. Haimberger, S. B. Healy, H. Hersbach, E. V. Hólm, L. Isaksen, P. Kållberg, M. Köhler, M. Matricardi, A. P. McNally, B. M. Monge-Sanz, J.-J. Morcrette, B.-K. Park, C. Peubey, P. de Rosnay, C. Tavalato, J.-N. Thépaut, F. Vitart, The ERA-Interim reanalysis: Configuration and performance of the data assimilation system. *Q. J. Roy. Meteorol. Soc.* **137**, 553–597 (2011).
37. A. H. Fink, D. G. Vincent, P. M. Reiner, P. Speth, Mean state and wave disturbances during phases I, II, and III of GATE based on ERA-40. *Mon. Weather Rev.* **132**, 1661–1683 (2004).
38. S. K. Kimball, M. S. Mulekar, A 15-year climatology of North Atlantic tropical cyclones. Part I: Size Parameters. *J. Climate* **17**, 3555–3575 (2004).
39. C. Xu, Y. Ma, K. Yang, C. You, Tibetan Plateau impacts global dust transport in the upper troposphere. *J. Climate* **31**, 10.1175/JCLI-D-17-0313.1 (2018).
40. T. Takemi, Explicit simulations of convective-scale transport of mineral dust in severe convective weather. *J. Meteorol. Soc. Jpn. Ser. II* **83A**, 187–203 (2005).
41. K. Sauter, T. S. L'Ecuyer, Observational evidence for the vertical redistribution and scavenging of Saharan dust by tropical cyclones. *Geophys. Res. Lett.* **44**, 6421–6430 (2017).
42. M. Peters, G. Tetzlaff, The structure of West African Squall Lines and their environmental moisture budget. *Meteorol. Atmos. Phys.* **39**, 74–84 (1988).
43. D. Goossens, Z. Y. Offer, Wind tunnel and field calibration of six aeolian dust samplers. *Atmos. Environ.* **34**, 1043–1057 (2000).
44. D. Goossens, Z. Offer, G. London, Wind tunnel and field calibration of five aeolian sand traps. *Geomorphology* **35**, 233–252 (2000).
45. M. Van der Does, G. J. A. Brummer, L. F. Korte, J. B. W. Stuut, Seasonality in Saharan dust particle characteristics across the Atlantic Ocean: transport versus deposition. Chapter 6, PhD Thesis: M. van der Does, *Saharan Dust from a Marine Perspective: Transport and Deposition Along a Transect in the Atlantic Ocean* (Vrije Universiteit Amsterdam, 2018).
46. H. Wernli, H. C. Davies, A lagrangian-based analysis of extratropical cyclones. I: The method and some applications. *Q. J. Royal Meteorol. Soc.* **123**, 467–489 (1997).
47. M. Sprenger, H. Wernli, The LAGRANTO Lagrangian analysis tool – version 2.0. *Geosci. Model Dev.* **8**, 2569–2586 (2015).
48. C. A. Frieze, M. van der Does, U. Merkel, M. H. Iversen, G. Fischer, J.-B. W. Stuut, Environmental factors controlling the seasonal variability in particle size distribution of modern Saharan dust deposited off Cape Blanc. *Aeolian Res.* **22**, 165–179 (2016).
49. M. Klose, Y. Shao, M. K. Karremann, A. H. Fink, Sahel dust zone and synoptic background. *Geophys. Res. Lett.* **37**, 10.1029/2010GL042816 (2010).
50. E. A. Afiesimama, Annual cycle of the mid-tropospheric easterly jet over West Africa. *Theor. Appl. Climatol.* **90**, 103–111 (2007).
51. “U.S. Standard Atmosphere” (National Oceanic and Atmospheric Administration, and National Aeronautics and Space Administration, 1976); <https://ntrs.nasa.gov/search.jsp?R=19770009539>

Acknowledgments: The captains, crews, and scientists of RV Pelagia cruises 64PE378 and 64PE395, RRS James Cook cruise JC134, and NIOZ technicians are thanked for deployment and retrieval of the dust-collecting buoys. We thank J. Fyfe and three anonymous reviewers for their thoughtful comments that helped improve this manuscript. **Funding:** This project was funded by the Netherlands Organisation for Scientific Research (NWO; project no. 822.01.008, TRAFFIC) and the European Research Council (ERC; project no. 311152, DUSTTRAFFIC), both awarded to J.-B.W.S. P.Z. is funded through subproject C4 “Coupling of planetary-scale Rossby wave trains to local extremes in heat waves” of the Transregional Collaborative Research Center SFB/TRR 165 “Waves to Weather,” funded by the German Research Foundation (DFG). **Author contributions:** J.-B.W.S. led the project and designed the study. M.v.d.D. processed and analyzed the samples. P.K. coordinated the discussion. P.Z. performed the trajectory calculations, and R.G.H. calculated the charge effects. M.v.d.D. wrote the paper, with input from the other authors. **Competing interests:** The authors declare that they have no competing interests. **Data and materials availability:** All data needed to evaluate the conclusions in the paper are present in the paper and/or the Supplementary Materials. Additional data related to this paper may be requested from the authors.

Submitted 24 May 2018
Accepted 8 November 2018
Published 12 December 2018
10.1126/sciadv.aau2768

Citation: M. van der Does, P. Knippertz, P. Zschenderlein, R. Giles Harrison, J.-B. W. Stuut, The mysterious long-range transport of giant mineral dust particles. *Sci. Adv.* **4**, eaau2768 (2018).

The mysterious long-range transport of giant mineral dust particles

Michèle van der Does, Peter Knippertz, Philipp Zschenderlein, R. Giles Harrison and Jan-Berend W. Stuut

Sci Adv 4 (12), eaau2768.
DOI: 10.1126/sciadv.aau2768

ARTICLE TOOLS

<http://advances.sciencemag.org/content/4/12/eaau2768>

SUPPLEMENTARY MATERIALS

<http://advances.sciencemag.org/content/suppl/2018/12/10/4.12.eaau2768.DC1>

REFERENCES

This article cites 41 articles, 0 of which you can access for free
<http://advances.sciencemag.org/content/4/12/eaau2768#BIBL>

PERMISSIONS

<http://www.sciencemag.org/help/reprints-and-permissions>

Use of this article is subject to the [Terms of Service](#)

Science Advances (ISSN 2375-2548) is published by the American Association for the Advancement of Science, 1200 New York Avenue NW, Washington, DC 20005. 2017 © The Authors, some rights reserved; exclusive licensee American Association for the Advancement of Science. No claim to original U.S. Government Works. The title *Science Advances* is a registered trademark of AAAS.